Finite element replication of acoustic Dirac-like cone and double zero refractive index

Akash Nivarthi, Chirag Gokani, Ryan Whitney

Acoustic Metamaterials, Fall 2021

Abstract

Dubois et al. reported the "the first experimental realization of an impedance matched acoustic double zero refractive index material"[1] in 2017. In this paper, finite element methods (FEM) are used to replicate the quasi-2D acoustic metamaterial (AMM) that Dubois et al. claim to host double-zero (DZ) properties. The dispersion relation generated by FEM shows that the AMM hosts a Dirac-like cone, a feature in the dispersion relation that induces a simultaneously vanishing compressibility and density.

Section (1) focuses on how a material's effective density and compressibility affect the magnitude and direction of wave propagation. Section (2) introduces the concept of the Dirac cone and Dirac point from the perspective of condensed matter physics. Section (3) reveals how the Dirac-like cone in acoustics relates to the Dirac cone in condensed matter physics. Section (4) describes the dimensions of the DZ AMM, and section (5) presents the FEM replication. Finally, section (6) offers a larger perspective and a sample implementation of DZ AMMs.

1 Introduction

The phase speed of a material is given by $c_{\text{phase}} = \pm(\chi\rho)^{-1/2}$, where χ is the compressibility and ρ is the density; engineering materials that explore the limits of c_{phase} thus requires knowledge of these parameters.[2] Since this work focuses on the $c_{\text{phase}} \to +\infty$ limit, constraints on the corresponding compressibility and density are derived.

A progressive plane pressure wave that propagates at the desired c_{phase} is given by

$$p(\boldsymbol{x}, t) = p \exp j(\omega t - \boldsymbol{k} \cdot \boldsymbol{x}) \tag{1}$$

The intensity of this progressive plane wave is $\boldsymbol{I} = I\boldsymbol{n}_E$, where $\boldsymbol{n}_E$ is a unit vector pointing in the direction that the intensity propagates. Assuming a complex wave vector, $\boldsymbol{k} = \boldsymbol{k}' - j\boldsymbol{\alpha}$, where $\boldsymbol{k}' = \frac{\omega}{|c_{\text{phase}}|}\boldsymbol{n}_{\text{phase}}$, $\boldsymbol{n}_{\text{phase}}$ is a unit vector pointing in the direction of propagation, and $\boldsymbol{\alpha}$ is the attenuation coefficient, then waves obeying $c_{\text{phase}} \to +\infty > 0$ will satisfy[3]

$$\boldsymbol{k}' \cdot \boldsymbol{I} > 0 \implies \frac{\omega}{|c_{\text{phase}}|}\boldsymbol{n}_{\text{phase}} \cdot I\boldsymbol{n}_E > 0 \tag{2}$$

Now denoting the velocity as $\boldsymbol{v}$, consider the conservation of linear momentum,[4]

$$\boldsymbol{\nabla} p = -\rho \cdot \dot{\boldsymbol{v}} \tag{3}$$

Upon substitution of equation (1), equation (3) becomes

$$j\boldsymbol{k}p = j\omega\rho\boldsymbol{v} \implies \boldsymbol{v} = \frac{\boldsymbol{k}}{\omega\rho}p$$

Recalling that the intensity is given in terms of pressure and velocity by[5] $\boldsymbol{I} = \frac{1}{2}\text{Re}(p\boldsymbol{v}^*)$, the intensity can now be found as a function of the pressure:

$$\boldsymbol{I} = \frac{1}{2}|p|^2 \,\text{Re}\left(\frac{\boldsymbol{k}}{\omega\rho}\right) \tag{4}$$

Combining equations (2) and (4) gives the inequality

$$\left(\frac{\omega}{|c_{\text{phase}}|}\boldsymbol{n}_{\text{phase}}\right)\left(\frac{1}{2}|p|^2 \,\text{Re}\left(\frac{\boldsymbol{k}}{\omega\rho}\right)\right) > 0 \tag{5}$$

Since $\boldsymbol{k}$ and $\boldsymbol{\alpha}$ are parallel for so-called homogeneous waves, $\boldsymbol{n}_{\text{phase}} \cdot \boldsymbol{k} = k = \frac{\omega}{|c_{\text{phase}}|}$. Then, equation (5) becomes

$$\frac{|p|^2}{2|c_{\text{phase}}|^2}\left(\frac{\omega}{\rho}\right) > 0 \tag{6}$$

Since $|p|^2, |c_{\text{phase}}|$, and ω are positive quantities, $\rho > 0$; since $c_{\text{phase}} = (\chi\rho)^{-1/2}$ must be a real quantity, $\chi > 0$, too. Further noting that $c_{\text{phase}} \to \infty$ as $\chi\rho$ vanishes,

$$\chi, \rho \to 0^+,$$

hence "double-zero" metamaterials. Note that the $\chi \to 0^\pm, \rho \to 0^\mp$ limits correspond to an infinite imaginary phase speed and hence evanescent wave propagation, and that the $\chi, \rho \to 0^-$, limit corresponds to a negative infinite phase speed.

It is also possible to achieve infinite phase speed for so-called "single-zero" metamaterials, in which χ (ρ) vanishes while ρ (χ) is finite. However, such metamaterials have little practical value. To see why, note that the impedance of a plane wave in the single-zero metamaterial is $Z = \rho c$. Upon substitution of $c = (\chi\rho)^{-1/2}$,

$$Z = \sqrt{\frac{\rho}{\chi}}$$

Evidently, the impedance is infinite (zero) when χ (ρ) vanishes while ρ (χ) is finite. Suppose an plane pressure wave traveling in a waveguide experiencing an impedance Z_{wg} is incident on this metamaterial. The transmission coefficient is then[6]

$$\begin{aligned} T &= \frac{2Z}{Z + Z_{\text{wg}}} \\ &= \begin{cases} 2, & Z \to \infty \implies R = -1 \\ 0, & Z \to 0 \implies R = 1 \end{cases} \end{aligned}$$

where R is the pressure reflection coefficient. So for single-zero metamaterials, the incident sound is totally reflected, either out-of-phase (when χ vanishes and ρ is finite) or in-phase (when χ is finite and ρ vanishes). In either case, single-zero metamaterials reflect the incident sound field due to this so-called "impedance mismatch" with the background material, making their properties hard to measure. DZ AMMs do not have this problem.[7]

2 Inspiration from condensed matter physics

The realization of a double-zero AMM draws on the earlier-realized double-zero photonic crystal. Photons obey[8]

$$\mu\epsilon\frac{\partial^2 \boldsymbol{E}}{\partial t^2} - \nabla^2 \boldsymbol{E} = 0 \tag{7}$$

The solution $\boldsymbol{E}$ to this 3D wave equation travels at $c_{\text{phase}} = \pm(\mu\epsilon)^{-1/2}$. Just as $c_{\text{phase}} = (\chi\rho)^{-1/2} \to \infty$ for $\chi, \rho \to 0^+$, $c_{\text{phase}} \to \infty$ for $\mu, \epsilon \to 0^+$.

Huang et al., whose approach for a DZ photonic crystal is adopted by Dubois et al., note that a Dirac cone that occurs at at the Brilloiun zone (BZ) edge "cannot be mapped to a zero-refractive-index system."[9] Instead, effective-zero properties can be realized by a Dirac cone at the Γ point ($\boldsymbol{k} = 0$), the BZ center. Achieving a Dirac cone at the Γ point, which requires the crossing of two locally linear dispersions, is difficult, however, because dispersion relations at the BZ center are generally quadratic.

One of Hamilton's equations, $\frac{\partial \mathcal{H}}{\partial \boldsymbol{p}} = \frac{\mathrm{d}\boldsymbol{r}}{\mathrm{d}t}$, constrains the effective parameters for a linear dispersion relation in a photonic system. Interpreting $\frac{\mathrm{d}\boldsymbol{r}}{\mathrm{d}t}$ as the group velocity $\boldsymbol{v}_{\text{group}}$ of a wave packet and writing $\boldsymbol{p} = \hbar\boldsymbol{q}$,[10] Hamilton's equation becomes[11]

$$\boldsymbol{v}_{\text{group}} = \frac{1}{\hbar}\boldsymbol{\nabla}_q E$$

Taking the time derivative of the group velocity gives the group acceleration, $\boldsymbol{a}$. Switching to index notation,

$$\begin{aligned} a_\alpha = \frac{\mathrm{d}v_{\text{group},\alpha}}{\mathrm{d}t} &= \frac{1}{\hbar}\frac{\mathrm{d}}{\mathrm{d}t}\left(\frac{\partial E(q)}{\partial q_\alpha}\right) \\ &= \frac{1}{\hbar}\sum_\beta \frac{\partial q_\beta}{\partial t}\frac{\partial}{\partial q_\beta}\left(\frac{\partial E(q)}{\partial q_\alpha}\right) \\ &= \frac{1}{\hbar^2}\sum_\beta F_\beta \frac{\partial^2 E(q)}{\partial q_\beta \partial q_\alpha} \qquad \text{(group acceleration)} \end{aligned}$$

where the chain rule is used in the second line, Newton's second law is used in the third line, and where F_β are components of the force. Recongnizing the (group acceleration) to be of the form $\boldsymbol{a} = \boldsymbol{F}/m$, we identify the effective mass in terms of its reciprocal:

$$\frac{1}{m_{\beta\alpha}} = \frac{1}{\hbar^2}\frac{\partial^2 E(q)}{\partial q_\beta \partial q_\alpha} \tag{8}$$

Apparently, the curvature of the dispersion relation $E(q)$ is proportional to the inverse of the elements of the mass matrix. Specifically, for the dispersion relation $E(q)$ to be linear, $\frac{\partial E(q)}{\partial q}$ is a constant, so the effective mass goes to 0. This constraint, along with the relativistic constraint of infinite phase speeds and the quantum mechanical constraint of $\hbar \neq 0$, suggests that a photonic system featuring linear dispersions is governed by a massless, relativistic, and quantum mechanical equation.[12] The massless Dirac equation satisfies these limits:[13]

$$\begin{pmatrix} 0 & -j\left(\frac{\partial}{\partial x} - j\frac{\partial}{\partial y}\right) \\ -j\left(\frac{\partial}{\partial x} + j\frac{\partial}{\partial y}\right) & 0 \end{pmatrix}\begin{pmatrix} E_{z,1} \\ E_{z,2} \end{pmatrix} = k(\omega)\begin{pmatrix} E_{z,1} \\ E_{z,2} \end{pmatrix} \tag{massless Dirac equation}$$

Since we are interested in a linear dispersion, we Taylor expand the eigenvalues of the (massless Dirac equation) about the Dirac frequency ω_D:

$$k(\omega) = k(\omega_D) + (\omega - \omega_D)\left.\frac{\partial k}{\partial \omega}\right|_{\omega=\omega_D} + \mathcal{O}(\omega^2)$$

Note that $k(\omega_D) = \frac{2\pi f_D}{c_{\text{phase}}} = 0$ because the phase speed is infinite at the Dirac point, and that $\left.\frac{\partial k}{\partial \omega}\right|_{\omega=\omega_D} = 1/v_{\text{group}}$. Then the (massless Dirac equation) becomes

$$\begin{pmatrix} 0 & -jv_{\text{group}}\left(\frac{\partial}{\partial x} - j\frac{\partial}{\partial y}\right) \\ -jv_{\text{group}}\left(\frac{\partial}{\partial x} + j\frac{\partial}{\partial y}\right) & 0 \end{pmatrix}\begin{pmatrix} E_{z,1} \\ E_{z,2} \end{pmatrix} = (\omega - \omega_D)\begin{pmatrix} E_{z,1} \\ E_{z,2} \end{pmatrix} \tag{9}$$

and the eigenvalues become

$$\omega - \omega_D = \pm v_{\text{group}} k(\omega) + \mathcal{O}(k^2) \tag{10}$$

The two eigenfunctions that correspond to these frequencies have linear dispersions and opposite group velocities. Section (3) shows that the DZ AMM obeys a 3×3 eigenvalue problem, two eigenvalues of which have the same leading linear term as equation (10).

To transition to the next section, a comparison is drawn between the parameters that give rise to the Dirac cone in condensed matter physics and the Dirac-like cone in acoustics:

	Condensed matter physics	**Acoustics**
Classical wave equation	$\mu\epsilon\frac{\partial^2 \boldsymbol{E}}{\partial t^2} - \nabla^2 \boldsymbol{E} = 0$	$\chi\rho\frac{\partial^2 p}{\partial t^2} - \nabla^2 p = 0$
Double-zero parameters	μ, ϵ	χ, ρ
Dispersion relation	$E(q)$	$\omega(k)$
Number of eigenvalues	2	3
Effectively massless	✓	✓
Relativistic	✓	✗
Quantum mechanical	✓	✗

3 Multiple Scattering Theory

Scattering theory is used to derive an eigenvalue equation analogous to equation (9). Since the scattering objects are roughly on the order of a wavelength, Mie scattering is used, which solves the Helmholtz equation in spherical coordinates by separation-of-variables. Huang et al. calculate the coefficients that determine the scattered field amplitudes $b_m(i)$ using P.C. Waterman's **T**-matrix technique, which reduces Mie scattering to[14]

$$b_m(i) = D_m(i) \sum_{j \neq i} \sum_n G_{mn}(i,j) b_n(j) \tag{11}$$

Equation (11) gives the Mie scattering coefficients $b_m(i)$ in terms of the **T**-matrix coefficients $D_m(i)$. $G_{mn}(i,j)$ are the elements of the matrix that transforms a scattered wave having an angular momentum number n for the jth scatterer into an incident wave having angular momentum number m for the ith scatterer. The index m is the angular momentum number; specifically, $m = 0$ corresponds to the monopolar mode, and $m = \pm 1$ corresponds to the dipolar mode. Invoking Bloch's theorem,[15] $b_m(i) = b_m e^{i\boldsymbol{k}\cdot\boldsymbol{R}_i}$, equation (11) becomes

$$b_m = D_m \sum_n S_{n-m}(-1)^{n-m} b_n \tag{12}$$

where S_{n-m} is the lattice sum. S_n is given by Huang et al. in reciprocal space in terms of the 2D unit cell area Ω, the spacing between nearest neighbors r_m, Bessel functions of the first kind J_α, and Hankel functions of the first kind $H^{(1)}$:

$$S_n = \frac{4i^{n+1}k_0}{\Omega} \sum_{G_i} \frac{J_{n+1}(k_{G_i} r_m)}{J_{n+1}(k_0 r_m)} \frac{e^{in\phi_{G_i}}}{k_{G_i}(k_0^2 - k_{G_i}^2)} - \frac{H_1^{(1)}(k_0 r_m) + 2i/(\pi k_0 r_m)}{J_1(k_0 r_m)} \delta_{n0} \tag{13}$$

Limiting ourselves to the subspace spanned by monopolar ($m = 0$) and dipolar ($m = \pm 1$) modes, equation 12 becomes

$$\begin{pmatrix} S_0 - 1/D_{-1} & -S_1 & S_2 \\ -S_1 & S_0 - 1/D_0 & -S_1 \\ S_{-2} & -S_{-1} & S_0 - 1/D_1 \end{pmatrix} \begin{pmatrix} b_{-1} \\ b_0 \\ b_1 \end{pmatrix} = \mathbf{0} \tag{14}$$

Since $S_{-m} = -S_m^*$, the matrix above is anti-Hermitian, similar to the Dirac operator. Further, by cylindrical symmetry, $D_1 = D_{-1}$ at the Γ-point.

Since a dispersion relation near the Γ-point is desired, a small wavenumber Taylor-expansion for the matrix elements $S_0 - 1/D_0$, $S_0 - 1/D_{\pm 1}$, $S_{\pm 1}$, and $S_{\pm 2}$ is taken. Leaving the Taylor expansions of equation (13) to the Supplementary Information of the Huang et al. paper, the results are written in terms of functions $A_0(\omega)$, $A_1(\omega)$, $B(\omega)$, $C_1(\omega)$, and $C_2(\omega, \phi_k)$:

$$\begin{aligned} S_0 - 1/D_0 &\simeq i(A_0(\omega) + B(\omega)\delta k^2) \\ S_0 - 1/D_{\pm 1} &\simeq i(A_1(\omega) + B(\omega)\delta k^2) \\ S_1 &\simeq C_1(\omega)\delta k e^{i\phi_k} \\ S_2 &\simeq C_2(\omega, \phi_k)\delta k^2 \end{aligned} \tag{Small wavenumber eqs.}$$

Note that *at* the Γ-point, $\delta k = 0$, which means that $S_{\pm 1} = S_{\pm 2} = 0$. Then the off-diagonal elements in equation (14) vanish, giving independent equations:

$$\begin{pmatrix} S_0 - 1/D_{-1} & 0 & 0 \\ 0 & S_0 - 1/D_0 & 0 \\ 0 & 0 & S_0 - 1/D_1 \end{pmatrix} \begin{pmatrix} b_{-1} \\ b_0 \\ b_1 \end{pmatrix} = \mathbf{0} \tag{15}$$

For non-trivial (non-quiet) solutions, these three equations imply

$$\begin{aligned} S_0 - 1/D_{-1} &= 0 \\ S_0 - 1/D_0 &= 0 \\ S_0 - 1/D_1 &= 0 \end{aligned}$$

Since $D_1 = D_{-1}$ at the Γ-point, the first and third equations above are equivalent; solving either for frequency gives the dipolar eigenfrequency ω_d. Meanwhile, the second equation for frequency gives the monopolar eigenfrequency ω_m.

3.1 The general case: $\omega_m \neq \omega_d$

A small ω Taylor expansion is taken of the first and third small wavenumber equations about ω_d and of the second equation about ω_m:

$$\begin{aligned} S_0 - 1/D_0 &\simeq i\left(\tfrac{\partial A_0}{\partial \omega}(\omega - \omega_m) + B(\omega)\delta k^2\right) \\ S_0 - 1/D_{\pm 1} &\simeq iA_1(\omega) \end{aligned}$$

Substituting the above, as well as $S_1 \simeq C_1 \delta k e^{i\phi_k}$ and $S_2 \simeq C_2 \delta k^2$, into equation (14),

$$\begin{pmatrix} iA_1 & -C_1\delta k e^{i\phi_k} & C_2\delta k^2 \\ C_1\delta k e^{i\phi_k} & i(\frac{\partial A_0}{\partial \omega}(\omega - \omega_m) + B\delta k^2) & -C_1\delta k e^{i\phi_k} \\ -C_2^*\delta k^2 & C_1\delta k e^{-i\phi_k} & iA_1 \end{pmatrix} \begin{pmatrix} b_{-1} \\ b_0 \\ b_1 \end{pmatrix} = \mathbf{0} \tag{16}$$

Since the region of interest is for small ω, the functions $\frac{\partial A_0}{\partial \omega}$, A_1, B, C_1, and C_2 are now treated as constant coefficients. Equation (16) has nontrivial solutions when the determinant of the 3×3 matrix vanishes. Evaluating the determinant gives the characteristic equation $\frac{\partial A_0}{\partial \omega}(\omega - \omega_m) + B\delta k^2 = 0$, which is the dispersion relation for the monopolar band.

Similarly, performing a small ω approximation of the the (Small wavenumber equations) near ω_d,

$$
\begin{aligned}
S_0 - 1/D_{\pm 1} &\simeq i\left(\frac{\partial A_1}{\partial \omega}(\omega - \omega_d) + B(\omega)\delta k^2\right) \\
S_0 - 1/D_0 &\simeq iA_0(\omega)
\end{aligned}
$$

Substituting the above, as well as $S_1 \simeq C_1 \delta k e^{i\phi_k}$ and $S_2 \simeq C_2 \delta k^2$, into equation (14),

$$
\begin{pmatrix}
i(\frac{\partial A_1}{\partial \omega}(\omega - \omega_d) + B\delta k^2) & -C_1\delta k e^{i\phi_k} & C_2 \delta k^2 \\
C_1 \delta k e^{i\phi_k} & iA_0 & -C_1 \delta k e^{i\phi_k} \\
-C_2^* \delta k^2 & C_1 \delta k e^{-i\phi_k} & i(\frac{\partial A_1}{\partial \omega}(\omega - \omega_d)
\end{pmatrix}
\begin{pmatrix} b_{-1} \\ b_0 \\ b_1 \end{pmatrix} = \mathbf{0} \tag{17}
$$

Equation (17) has nontrivial solutions when the determinant of the 3×3 matrix vanishes. Evaluating the determinant gives the characteristic equation $\frac{\partial A_1}{\partial \omega}(\omega - \omega_m) + B\delta k^2 = 0$, which is the dispersion relation for the dipolar band.

Note that for $\omega_m \neq \omega_d$ both monopolar and dipolar bands are quadratic in wavenumber. That is, a Dirac-like cone and an associated Dirac point does not exist at the Γ-point if $\omega_m \neq \omega_d$.

3.2 The case of accidental degeneracy: $\omega_m = \omega_d \equiv \omega_D$

The process is repeated for the case of accidental degeneracy. Performing a small ω approximation of the (Small wavenumber equations) near ω_D,

$$
\begin{aligned}
S_0 - 1/D_0 &\simeq i\left(\frac{\partial A_0}{\partial \omega}(\omega - \omega_D) + B(\omega)\delta k^2\right) \\
S_0 - 1/D_{\pm 1} &\simeq i\left(\frac{\partial A_1}{\partial \omega}(\omega - \omega_D) + B(\omega)\delta k^2\right)
\end{aligned}
$$

Substituting the above, as well as $S_1 \simeq C_1 \delta k e^{i\phi_k}$ and $S_2 \simeq C_2 \delta k^2$, into equation (14),

$$\begin{pmatrix} i\left(\frac{\partial A_1}{\partial\omega}(\omega-\omega_D)+B\delta k^2\right) & -C_1\delta k e^{i\phi_k} & C_2\delta k^2 \\ C_1\delta k e^{i\phi_k} & i\left(\frac{\partial A_1}{\partial\omega}(\omega-\omega_D)+B(\omega)\delta k^2\right) & -C_1\delta k e^{i\phi_k} \\ -C_2^*\delta k^2 & C_1\delta k e^{-i\phi_k} & i\left(\frac{\partial A_1}{\partial\omega}(\omega-\omega_D)+B\delta k^2\right) \end{pmatrix}\begin{pmatrix} b_{-1} \\ b_0 \\ b_1 \end{pmatrix} = \mathbf{0} \tag{18}$$

As before, equation (18) has nontrivial solutions when the determinant of the 3×3 matrix vanishes. Notating $\omega - \omega_D = \delta\omega$ and evaluating the determinant gives following cubic equation:

$$\begin{aligned} &-\left(\frac{\partial A_1}{\partial\omega}\delta\omega+B\delta k^2\right)^2\left(\frac{\partial A_0}{\partial\omega}\delta\omega+B\delta k^2\right)+ \\ &+2\left(\frac{\partial A_1}{\partial\omega}+B\delta k^2\right)C_1^2\delta k^2+\left(\frac{\partial A_1}{\partial\omega}\delta\omega+B\delta k^2\right)|C_2|^2\,\delta k^4-2\ \mathrm{Im}\ (C_2^*e^2 i\phi_k)C_1^2\delta k^4=0 \end{aligned}$$

Noting that $v_{\text{group}} = \frac{\sqrt{2}|C_1|}{\sqrt{\frac{\partial A_1}{\partial\omega}\frac{\partial A_0}{\partial\omega}}}$, the three solutions of the cubic equation are

$$\begin{aligned} \omega_1 - \omega_D &= 0 + \mathcal{O}(\delta k^2) \\ \omega_{2,3} - \omega_D &= \pm v_{\text{group}}\delta k + \mathcal{O}(\delta k^2) \end{aligned}$$

In contrast to the quadratic dispersion relations near the Γ-point found in section (3.1), the accidental degeneracy of the monopolar and dipolar modes forces these dispersions to be linear and cross at a point. Also note that the Dispersion corresponding to the dipolar modes is of the same form as equation (10), the dispersion predicted by the massless Dirac equation.

4 Dimensions of the double-zero acoustic metamaterial

The appropriate dimensions for the cylindrical scatterers and the square lattice can be found using equation (13), which includes Ω, the area of the cylindrical scatterers, and r_m, the

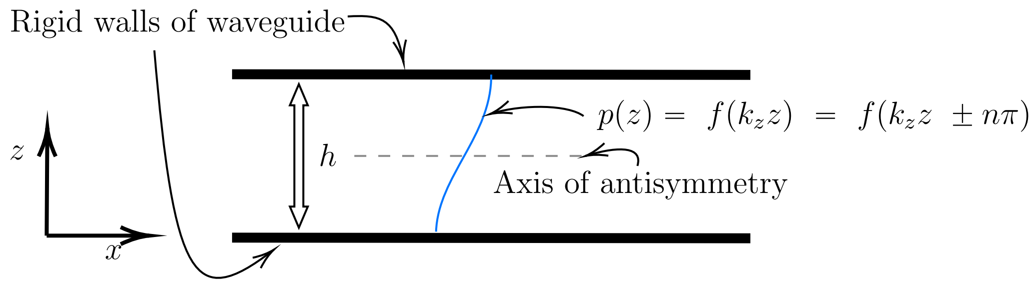

Figure 1: This schematic shows the standing-wave profile of the lowest-order waveguide mode.

spacing between nearest neighbors. The diamater of the cylindrical scatterers is $2\sqrt{\Omega/\pi}$, and the square unit cell side length is r_m. The thickness of the waveguide and height of the cylindrical scatterers is arbitrary, as long as the chosen thickness and height of the scatterers are such that the operating frequency lies within only one waveguide mode. The frequencies used by Dubois et al. indeed lie within the lowest-order waveguide mode.[16]

Note that the pressure amplitude attains a maximum at the walls of the waveguide because they are rigid. The lowest-order pressure mode along the z-axis is therefore a function $p(z)$ that is anti-symmetric about the waveguide's center, as shown in figure (1). Any antisymmetric function with spatial periodicity $k_z = \frac{\pi}{h}$ satisfies the boundary conditions. Noting in the quasi-2D geometry that $k^2 = \frac{\omega^2}{c_0^2} = k_x^2 + k_z^2$, where $c_0 = 343$ m/s,

$$k_x = \frac{\omega}{c} = \sqrt{k^2 - k_z^2} = \sqrt{\frac{\omega^2}{c_0^2} - \frac{\pi^2}{h^2}} \tag{19}$$

Note that k_x is real for $\frac{\omega}{c} \geqslant \frac{\pi}{h}$, so the cut-on frequency of the first-order waveguide mode is

$$f_{\text{cut-on, 1}} = \frac{c_0}{2h} = \begin{cases} 17150 \text{ Hz}, \ h = 10 \text{ mm} \\ \\ 12250 \text{ Hz}, \ h = 14 \text{ mm} \end{cases}$$

Meanwhile, the second-order waveguide mode corresponds to a spatial periodicity of $k_z = \frac{2\pi}{h}$, so the corresponding cut-on frequency for this mode is

$$f_{\text{cut-on, 2}} = \frac{c_0}{h} = \begin{cases} 34300 \text{ Hz}, \ h = 10 \text{ mm} \\ 24500 \text{ Hz}, \ h = 14 \text{ mm} \end{cases}$$

The FEM sweeps 0 - 20 kHz and therefore operates in the first waveguide mode.[17]

5 FEM replication

5.1 Replica of Dubois et al. geometry

Dubois et al. gave the following dimensions for their geometry:

Parameter	**Dimension (mm)**
Diameter of cylindrical scatterers	16
Waveguide thickness	10
Height of cylindrical scatterers	14.5
Square unit cell side length	30

Figure (2) shows the replication of the unit cell geometry defined by Dubois et al. The unit cell was designed in SolidWorks and was imported into COMSOL for a pressure acoustics (frequency domain) study. Acrylic plastic was chosen as the material for the unit cell, matching the specifications of Dubois et al..

5.2 Band diagram

After applying a physics-controlled mesh to the unit cell and setting the element size set to "fine," an series of eigenfrequency studies were run. The first study found the eigenfrequencies at the Γ-point, and subsequent studies found the eigenfrequencies for wavenumbers Γ to M, Γ to X, and X to M. The data was exported and processed in MATLAB, where the solutions were "patched" together and plotted on a frequency versus k band diagram to match figure 2(a) from the Dubois et al. paper. The Γ-point ($\boldsymbol{k} = 0$) is the so-called "Brillouin zone center" and is therefore set at the center of the band diagram.

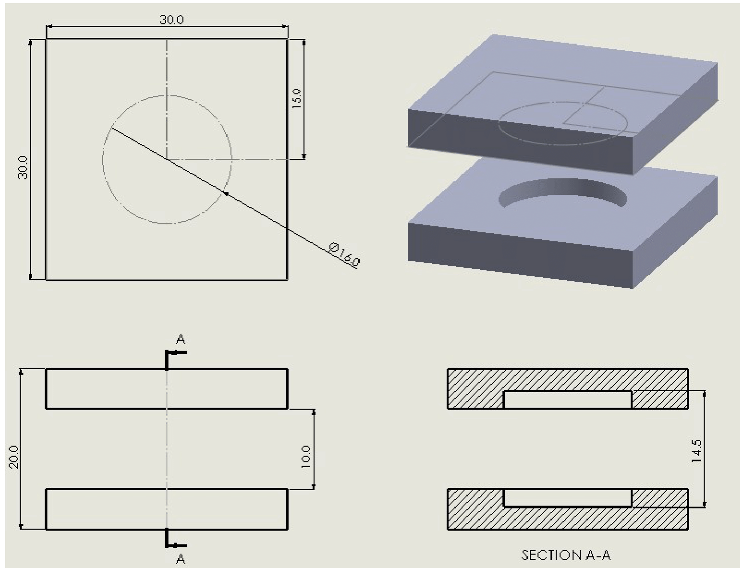

Figure 2: This figure shows the geometry of the unit cell, created in SolidWorks and then imported to COMSOL.

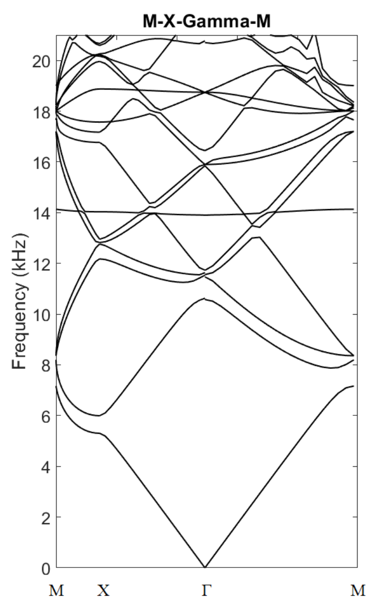

Figure 3: Above is the calculated band diagram, with data generated in COMSOL and patched together in MATLAB. The Dirac point occurs at the BZ center (the Γ point) at $1.87 * 10^4$ Hz.

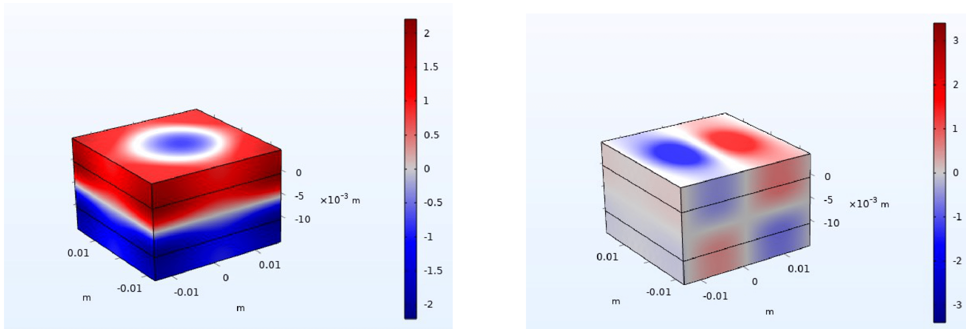

(a) Monopolar pressure field

(b) Dipolar pressure field

Figure 4: Above are the pressure fields calculated in COMSOL at the Dirac point of the degenerate monopolar and dipolar modes of the lowest-order waveguide mode

The Dirac-like cone occurs at the Γ-point for the frequency $1.87 * 10^4$ Hz, as reported in the original paper. Visually comparing figure (3) above to figure 2a of the Dubois et al. paper reveals a strong agreement of the results. The only apparent difference is due to the fact that Dubois et al. presented the band diagram for frequencies 0 - $2 * 10^4$ Hz, while the band diagram above sweeps frequencies 0 - $2.5 * 10^4$ Hz.

Figure (4) shows the pressure maps generated in COMSOL of the monopolar and dipolar modes on the unit cell. These figures match Dubois et al.'s figures 2c and 2d.

6 Future Directions

6.1 Engineering

Since the phase speed in a DZ AMM is infinite, wavefronts within these materials do not accumulate phases and therefore overcome diffraction. The effect is that sound can remain highly columnated within the AMM. There are ways to achieve the same effect in nonlinear acoustics (for example, a parametric array); what makes the DZ AMM remarkable is that this columnation is achieved in the linear regime. Further, the dimensions of the DZ AMM can be scaled to achieve columnated sound at any frequency, while the nonlinear technologies operate best at low frequencies (as they often involve the subtraction tones of two high frequencies).

One downside to DZ AMMs is that sound columnation is achieved at only one frequency, in contrast with nonlinear technologies like parametric arrays, whose transduction mechanism easily accommodates real-time frequency modulation. Applications of DZ AMMs are therefore inherently monochromatic. Fortunately, many acoustical applications are realized in the narrow band, including transformation acoustics, wavefront and dispersion engineering, phase matching, ultrasound medical imaging, and underwater communication, according to Dubois et al.

6.2 Physics research

Wang et al. describe how optical analogs are easier to work with than electronic systems: "Compare[d] with solids, optical systems offer a clean and easily controlled way to test theoretical predictions...[T]herefore establishing the optical analog of graphene wold open up the possibility to study condensed matter analogies in an optical way." Acoustics shares this ease of experiment and can serve the same purpose. Sensitive experiments assessing the dispersive properties of graphene and other condensed-matter materials hosting Dirac cones can indirectly be carried out using DZ AMMs.

Author Contributions

A.N. worked tirelessly in COMSOL to reproduce figure 2f in the Dubois et al. paper. The results had similar behavior, but the magnitude of the transmission coefficient was lower than 0.9. Although the transmission phenomenon was studied heavily by A.N., the group chose not to present this aspect of the work in the paper since the results did not those of Dubois et al. C.G. handled the analytical aspects of this work and wrote the paper. R.W. replicated the Dubois et al. experiment in COMSOL. He generated the band diagram and wrote the MATLAB script to process the COMSOL data.

Notes

[1]Dubois, M., Shi, C. Zhu, X., Wang, Y., Zhang, X. Observation of acoustic Dirac-like cone and double zero refractive index *Nature Communications.* **8**, 14871 (2017).

[2]Haberman, M, Guild, M. Acoustic Metamaterials. *Physics Today.* **69**, 42 (2016).

[3]"Positive phase speed" means that the intensity and the wave vector are parallel; "Negative phase speed" means that intensity and the wave vector are anti-parallel.

[4]Blackstock, D. Fundamentals of Physical Acoustics. *Wiley*, 67 (2000).

[5]Blackstock, D. Fundamentals of Physical Acoustics. *Wiley*, 50 (2000).

[6]Blackstock, D. Fundamentals of Physical Acoustics. *Wiley*, 110 (2000).

[7]DZ AMMs do not have this problem as long as both ρ and χ vanish at similar rates as functions of frequency.The normalized plots of $\rho(f)$ and $\chi(f)$ show that both vanish at very similar rates. See Dubois et al., Supplementary Figure 2.

[8]Photons are governed by Maxwell's equations, which, in the absence of charges and currents, read $\boldsymbol{\nabla} \cdot \boldsymbol{E} = 0, \boldsymbol{\nabla} \cdot \boldsymbol{B} = 0, \boldsymbol{\nabla} \times \boldsymbol{E} = -\frac{\partial \boldsymbol{B}}{\partial t}$, and $\boldsymbol{\nabla} \times \boldsymbol{B} = \mu\epsilon\frac{\partial \boldsymbol{E}}{\partial t}$. These four first-order equations can be combined into two second-order coupled PDEs by first taking the curl of the curl equations:

$$\boldsymbol{\nabla} \times \boldsymbol{\nabla} \times \boldsymbol{E} = -\boldsymbol{\nabla} \times \frac{\partial \boldsymbol{B}}{\partial t}$$
$$\boldsymbol{\nabla} \times \boldsymbol{\nabla} \times \boldsymbol{B} = \mu\epsilon \left(\boldsymbol{\nabla} \times \frac{\partial \boldsymbol{E}}{\partial t}\right)$$

Applying the identity $\boldsymbol{\nabla} \times \boldsymbol{\nabla} \times \boldsymbol{P} = \boldsymbol{\nabla} \left(\boldsymbol{\nabla} \cdot \boldsymbol{P}\right) - \nabla^2 \boldsymbol{P}$ the left-hand-side becomes

$$\begin{aligned} \boldsymbol{\nabla}\left(\boldsymbol{\nabla}\cdot\boldsymbol{E}\right)-\nabla^2\boldsymbol{E} &= -\boldsymbol{\nabla}\times\tfrac{\partial\boldsymbol{B}}{\partial t} \\ \boldsymbol{\nabla}\left(\boldsymbol{\nabla}\cdot\boldsymbol{B}\right)-\nabla^2\boldsymbol{B} &= \mu\epsilon\left(\boldsymbol{\nabla}\times\tfrac{\partial\boldsymbol{E}}{\partial t}\right) \end{aligned}$$

But invoking the divergence equations gives

$$\begin{aligned} \nabla^2\boldsymbol{E} &= \boldsymbol{\nabla}\times\tfrac{\partial\boldsymbol{B}}{\partial t} \\ -\nabla^2\boldsymbol{B} &= \mu\epsilon\left(\boldsymbol{\nabla}\times\tfrac{\partial\boldsymbol{E}}{\partial t}\right) \end{aligned}$$

We can simplify further, noting that

$$\begin{aligned} \boldsymbol{\nabla}\times\tfrac{\partial\boldsymbol{B}}{\partial t} &= \tfrac{\partial}{\partial t}\left(\boldsymbol{\nabla}\times B\right) \\ &= \mu\epsilon\tfrac{\partial^2\boldsymbol{E}}{\partial t^2} \end{aligned}$$

and

$$\begin{aligned} \boldsymbol{\nabla}\times\tfrac{\partial\boldsymbol{E}}{\partial t} &= \tfrac{\partial}{\partial t}\left(\boldsymbol{\nabla}\times E\right) \\ &= -\tfrac{\partial^2\boldsymbol{B}}{\partial t^2} \end{aligned}$$

The vector Laplacian equations then become

$$\begin{aligned} \mu\epsilon\tfrac{\partial^2\boldsymbol{E}}{\partial t^2}-\nabla^2\boldsymbol{E} &= 0 \\ \mu\epsilon\tfrac{\partial^2\boldsymbol{B}}{\partial t^2}-\nabla^2\boldsymbol{B} &= 0 \end{aligned}$$

[9]Huang, X., Lai, Y., Hang, Z. H., Zheng, H. Chan, C. T. Dirac cones induced by accidental degeneracy in photonic crystals and zero-refractive-index materials. *Nat. Mater.* **10**, 582–586 (2011).

[10]$\boldsymbol{q}$ is the so-called "crystal momentum."

[11]We have assumed that the Hamiltonian equals the total energy, i.e., that the fields are conservative. Dimensionally, our result makes sense: $\hbar$ is in Joule-seconds, the gradient with respect to the wave vector factors in meters, and energy is in Joules. The dimensions of $\frac{1}{\hbar}\boldsymbol{\nabla}_q E$ is therefore $[\mathrm{J}^{-1} \cdot \mathrm{s}^{-1}][m][J] = [m/s]$, which are the SI units of velocity.

[12]Wang, L., Wang, Z., Zhang, J. et al. Realization of Dirac point with double cones in optics *Optics Letters*, **34**, 2009.

[13]The massless Dirac equation can be formulated by first taking the Fourier transform of equation (7). Note that we are assuming polarity in the z-direction to make the analogy to the acoustical system in the Dubois et al. paper more direct.

$$\left(\frac{\partial^2}{\partial x^2} + \frac{\partial^2}{\partial y^2}\right) E_z(x, y, \omega) + k^2(\omega) E_z(x, y, \omega) = 0 \tag{20}$$

Recall that the x- and y-Pauli spin matrices are

$$\sigma_x = \begin{pmatrix} 0 & 1 \\ 1 & 0 \end{pmatrix}$$

$$\sigma_y = \begin{pmatrix} 0 & -j \\ j & 0 \end{pmatrix}$$

The Laplacian is factored in the style of P.A.M. Dirac. The Laplacian in the spin-$\frac{1}{2}$ basis equals Dirac's factored Laplacian:

$$
\begin{aligned}
\left(\tfrac{\partial^2}{\partial x^2}+\tfrac{\partial^2}{\partial y^2}\right)\mathbf{1} &\overset{?}{=} \left(\begin{pmatrix}0&1\\1&0\end{pmatrix}\tfrac{\partial}{\partial x}+\begin{pmatrix}0&-j\\j&0\end{pmatrix}\tfrac{\partial}{\partial y}\right)\left(\begin{pmatrix}0&1\\1&0\end{pmatrix}\tfrac{\partial}{\partial x}+\begin{pmatrix}0&-j\\j&0\end{pmatrix}\tfrac{\partial}{\partial y}\right)\\
&= \begin{pmatrix}0&1\\1&0\end{pmatrix}\begin{pmatrix}0&1\\1&0\end{pmatrix}\frac{\partial^2}{\partial^2 x}+\begin{pmatrix}0&1\\1&0\end{pmatrix}\begin{pmatrix}0&-j\\j&0\end{pmatrix}\frac{\partial^2}{\partial x\partial y}+\\
&+\begin{pmatrix}0&-j\\j&0\end{pmatrix}\begin{pmatrix}0&1\\1&0\end{pmatrix}\frac{\partial^2}{\partial x\partial y}+\begin{pmatrix}0&-j\\j&0\end{pmatrix}\begin{pmatrix}0&-j\\j&0\end{pmatrix}\frac{\partial^2}{\partial^2 y}\\
&= \begin{pmatrix}1&0\\0&1\end{pmatrix}\frac{\partial^2}{\partial^2 x}+\begin{pmatrix}j&0\\0&-j\end{pmatrix}\frac{\partial^2}{\partial x\partial y}+\begin{pmatrix}-j&0\\0&j\end{pmatrix}\frac{\partial^2}{\partial x\partial y}+\begin{pmatrix}1&0\\0&1\end{pmatrix}\frac{\partial^2}{\partial^2 y}\\
&= \begin{pmatrix}1&0\\0&1\end{pmatrix}\frac{\partial^2}{\partial^2 x}+\begin{pmatrix}1&0\\0&1\end{pmatrix}\frac{\partial^2}{\partial^2 y} \qquad (\checkmark)
\end{aligned}
$$

Therefore

$$
\left(\tfrac{\partial^2}{\partial x^2}+\tfrac{\partial^2}{\partial y^2}\right)\mathbf{1} = \left(\begin{pmatrix}0&1\\1&0\end{pmatrix}\tfrac{\partial}{\partial x}+\begin{pmatrix}0&-j\\j&0\end{pmatrix}\tfrac{\partial}{\partial y}\right)\left(\begin{pmatrix}0&1\\1&0\end{pmatrix}\tfrac{\partial}{\partial x}+\begin{pmatrix}0&-j\\j&0\end{pmatrix}\tfrac{\partial}{\partial y}\right)
$$

Equation (20) then becomes

$$
\left(\begin{pmatrix}0&1\\1&0\end{pmatrix}\tfrac{\partial}{\partial x}+\begin{pmatrix}0&-j\\j&0\end{pmatrix}\tfrac{\partial}{\partial y}\right)\left(\begin{pmatrix}0&1\\1&0\end{pmatrix}\tfrac{\partial}{\partial x}+\begin{pmatrix}0&-j\\j&0\end{pmatrix}\tfrac{\partial}{\partial y}\right)\begin{pmatrix}E_{z,1}\\E_{z,2}\end{pmatrix} = -k^2(\omega)\begin{pmatrix}E_{z,1}\\E_{z,2}\end{pmatrix}
$$

Since each of the matrix operators above (so-called “Dirac operators”) is a functional square root of the Laplacian, each one generates an eigenvalue of $\sqrt{-k^2(\omega)} = jk(\omega)$. Taking the functional square root of the above gives

$$\frac{1}{j}\begin{pmatrix} 0 & \frac{\partial}{\partial x} - j\frac{\partial}{\partial y} \\ \frac{\partial}{\partial x} + j\frac{\partial}{\partial y} & 0 \end{pmatrix}\begin{pmatrix} E_{z,1} \\ E_{z,2} \end{pmatrix} = k(\omega)\begin{pmatrix} E_{z,1} \\ E_{z,2} \end{pmatrix}$$

$$\begin{pmatrix} 0 & -j\left(\frac{\partial}{\partial x} - j\frac{\partial}{\partial y}\right) \\ -j\left(\frac{\partial}{\partial x} + j\frac{\partial}{\partial y}\right) & 0 \end{pmatrix}\begin{pmatrix} E_{z,1} \\ E_{z,2} \end{pmatrix} = k(\omega)\begin{pmatrix} E_{z,1} \\ E_{z,2} \end{pmatrix} \qquad \text{(massless Dirac equation)}$$

[14]Adapted from the *Supplementary Information* of the Huang et al. paper.

[15]In this section, we will switch to the $e^{i(kx-\omega t)}$ convention to match the paper by Huang et al.. The final result is entirely real, so comparison to the results in the previous section should be straightforward.

[16]The supplementary information includes important derivations and details about the experiment.

[17]Solving $\frac{\omega}{c} = \sqrt{\frac{\omega^2}{c_0^2} - \frac{\pi^2}{h^2}}$ for c, the phase speed of the lowest-order waveguide mode,

$$c = \frac{\omega}{k_x} = \left(\sqrt{\frac{1}{c_0^2} - \frac{\pi^2}{\omega^2 h^2}}\right)^{-1} \qquad \text{(Dubois et al. equation 1)}$$

This note was included for the sake of reproducing the only equation that appears in the Dubois et al. paper.